

Spontaneous magnetization in the dipolar Ising ferromagnet LiTbF_4

J. Als-Nielsen

Atomic Energy Commission Research Establishment Risø, 4000 Roskilde, Denmark

L. M. Holmes*

Eidgenössische Technische Hochschule, Zürich, Switzerland

F. Krebs Larsen

Aarhus University, 8000 Aarhus, Denmark

H. J. Guggenheim

Bell Laboratories, Murray Hill, New Jersey 07994

(Received 19 December 1974)

The spontaneous magnetization μ in Bohr magnetons below $T_C = 2.874$ K in LiTbF_4 has been measured by magnetic Bragg scattering of neutrons. The data were normalized by comparing the magnetic Bragg scattering to the nuclear Bragg scattering at $T > T_C$. The nuclear structure factors as well as the extinction corrections were determined at 295 and 100 K by a conventional neutron structure analysis from 304 and 196 nonsymmetry-related Bragg reflections, respectively. In the critical region $0.001 < 1 - T/T_C < 0.034$, the data obeyed the power law $\mu = (19 \pm 2)(1 - T/T_C)^{0.45 \pm 0.03}$. The saturation moment is $8.9\mu_B$.

I. INTRODUCTION

The most striking and fascinating aspect of critical phenomena is their universality. It appears that it is only the dimensionality (d) of the space in which the order parameter becomes more and more correlated as the critical temperature is approached and the number (n) of the order-parameter components that determine the critical behavior of any system. The strength and the range of interaction between the constituents is irrelevant for the critical behavior as long as it is finite. The reason is that the spatial correlation of the fluctuations will always exceed the interaction range by any prescribed value if the temperature is sufficiently close to T_C and details about the interaction range can then no longer be of importance in determining the critical behavior. Kadanoff showed that this picture immediately leads to relations between critical exponents,¹ the so-called scaling laws. With Wilson's work on critical phenomena² the Kadanoff picture is worked out in an ingenious way to a quantitative theory, the renormalization-group theory. Wilson found that mean-field or Landau critical behavior occurred for all four-dimensional systems with short-range interactions. In the theory the dimensionality d can formally be treated as a continuous variable, and Wilson and Fisher³ found corrections to the mean-field critical exponents by expanding in $\epsilon = 4 - d$. The renormalization-group theory is then the first theory explaining the universality of critical phenomena, and it is

possible in this theory to estimate the deviation of critical exponents from mean-field values although the precision is not as high as that obtainable from series expansion of, say, the susceptibility in terms of $1/T$ for *specific* simple models.

Most interestingly, Larkin and Khmel'nitskii⁴ found some years ago that apart from logarithmic corrections Landau critical behavior should occur in the $3d$, Ising ($n = 1$) dipolar-coupled ferromagnet. The same result was recently rederived by Aharony and Fisher⁵ using the Wilson renormalization-group technique. Around the same time it was discovered that LiTbF_4 very likely is an accurate realization in nature of that model system.^{6,7} In the preceding paper⁸ it was shown that subsequent high-precision experimental data are consistent with the statement that LiTbF_4 is a dipolar-coupled Ising ferromagnet, and the small exchange interactions were determined. In this paper we describe measurements of the spontaneous magnetization as determined by magnetic Bragg scattering of neutrons.

II. EXPERIMENTAL

A. Neutron-diffraction structure analysis: Extinction correction

The magnetic Bragg scattering is proportional to the squared spontaneous magnetization, and the scale factor can be found by comparing the magnetic intensity to the nuclear intensity utilizing the fact that 1 Bohr magneton has the same scattering power as a nucleus with scattering length 2.7 fm. This procedure presumes of course that the crystallographic structure factor is pre-

cisely known. Furthermore, it is presumed that attenuation of the beam due to the Bragg scattering is negligible. If this is not the case a correction must be determined, the so-called extinction correction.

In our experiment the crystallographic structure as well as the extinction correction were determined by a conventional neutron-diffraction structure analysis at 295 and 100 K,⁹ using a four-circle Hilger-Ferranti diffractometer operated at an incident wavelength of $\lambda = 1.070 \text{ \AA}$.

The structure of LiTbF_4 at both 295 and at 100 K is isomorphous with that of LiYbF_4 ,¹⁰ and so belongs to the tetragonal space group $I4_1/a$, with $Z = 4$. Lattice constants were determined from the angular positions of axial reflections, $a_0(295 \text{ K}) = 5.192(3) \text{ \AA}$; $c_0(295 \text{ K}) = 10.875(6) \text{ \AA}$; $a_0(100 \text{ K}) = 5.181(3) \text{ \AA}$; $c_0(100 \text{ K}) = 10.873(6) \text{ \AA}$. These may be compared with $a_0 = 5.200(5) \text{ \AA}$ and $c_0 = 10.89(1) \text{ \AA}$ reported previously¹¹ for polycrystalline LiTbF_4 .

At room temperature 1233 reflections with $\sin\theta/\lambda < 0.85$ were measured, of which 304 were unrelated by symmetry and of significant intensity. The internal consistency R factor, $\sum |F_{\text{obs}}^2 - \langle F_{\text{obs}}^2 \rangle| / \sum F_{\text{obs}}^2$, was 2.8%. 692 of the strongest intensities were also measured at 100 K,⁹ giving 196 independent reflections for least-squares analysis. The internal consistency R factor was 2.2%. The integrated intensities were evaluated by a method which divides the step-scanned profile into peak and background in such a way that the relative standard deviation based on counting statistics of the integrated intensity I_{hkl} is minimized.¹² The intensities from the 7-mm-diam spherical crystal were corrected for absorption by an analytical expression¹³ using a neutron absorption coefficient $\mu = 0.893 \text{ cm}^{-1}$ calculated from tabulated mass absorption coefficients.¹⁴ The intensities were reduced to squared structure amplitudes, $F_{\text{obs},hkl}^2$, in arbitrary units, by dividing with $\sin 2\theta_{hkl}$:

$$F_{\text{obs},hkl}^2 = I_{hkl} / \sin 2\theta_{hkl}. \quad (1)$$

The nuclear structure factor F_{hkl} is defined by

$$F_{hkl} = \sum_j b_j e^{2\pi i \vec{\tau}_{hkl} \cdot \vec{\rho}_j} e^{-2\pi^2 \vec{\tau}_{hkl} \underline{U}_j \vec{\tau}_{hkl}}. \quad (2)$$

Here b_j is the nuclear scattering amplitude of the atom located at the equilibrium position $\vec{\rho}_j$ in the unit cell. The thermal vibrations are taken into account by the second exponential function in Eq. (2), the Debye-Waller factor. The anisotropic vibrations of each atom in the unit cell is given by a 3×3 matrix \underline{U}_j .

The observed intensities are affected by extinction. The extinction coefficient E_{hkl} was approximated with the expression suggested by Zacharia-

sen¹⁵

$$E_{hkl}(g) \approx \left(1 + g \frac{2\bar{l}(\Theta_{hkl}) F_{hkl}^2}{V \sin 2\Theta_{hkl}} \right)^{-1/2}. \quad (3)$$

Here $\bar{l}(\Theta_{hkl})$ is the average length in the crystal of a ray scattered once through the angle $2\Theta_{hkl}$, V is $(a_0^2 c_0)^2 / \lambda^3$, and g is a dimensionless parameter to be least-squares fitted to the data. In the least-squares fitting the function

$$\sum_{hkl} w_{hkl} [N F_{\text{obs},hkl}^2 / E_{hkl}(g) - F_{hkl}^2]$$

was minimized with respect to the scale factor N , the atomic positions $\vec{\rho}_j$ and vibrations \underline{U}_j in F_{hkl}^2 and the extinction parameter g . The weights w_{hkl} would be I_{hkl}^{-1} if uncertainties derived solely from Poisson statistics, but in order not to overweight the intense but extinction-affected peaks, we used $w_{hkl}^{-1} = I_{hkl} + (0.02 I_{hkl})^2$. Also the scattering lengths of the atoms were included individually as variables in the least-squares refinement without significant improvement in the reliability index.

Results of the structure analysis are given in Table I. The Li^+ and Tb^{3+} ions occupy special positions (4a) and (4b) respectively, whereas the F^- ions are in the general positions (16f). The derived values of the F^- parameters in Table I deviate only slightly ($< 2\%$) from those found¹⁰ in LiYbF_4 . By comparing the values at 300 and 100 K we were able to estimate the values at 4 K simply by assuming that each ion is vibrating independently of the other ions in a harmonic oscillator potential. We find that the mean-squared vibration amplitudes decrease only by (1–2)% in going from 100 to 4 K. The best-fit value of the extinction parameter g implies an extinction coefficient versus $F_{hkl}^2 / \sin(2\theta)$ as shown in Fig. 1. The best-fit values of the scattering lengths are given in Table II. Our data are consistent with those recommended by the Neutron Diffraction Commission.¹⁶

Observed and calculated squared structure factors can be obtained by request to one of us (F. K. L.).

B. Intensity conversion to magnetization below T_C

We shall now return to the question of how we relate the observed magnetic Bragg scattering intensity below $T_C = 2.874 \text{ K}$ to the spontaneous magnetization μ . The extinction-free intensity above T_C is proportional to $F_{hkl}^2 / \sin 2\theta_{hkl}$ and below T_C to $(F_{hkl}^2 + F_{\text{magn}}^2) / \sin 2\theta_{hkl}$ with

$$F_{\text{magn}} = \mu \sum_j \beta_j e^{2\pi i \vec{\tau} \cdot \vec{\rho}_j} e^{-2\pi^2 \vec{\tau} \underline{U}_j \vec{\tau}} \times f(\vec{\tau}) \left(1 - \frac{\tau^2}{\tau^2} \right)^{1/2}. \quad (4)$$

TABLE I. Atomic positions $\vec{\rho}_j$ in fractions of the unit-cell edges and the mean-squared displacement matrix U_j , as defined in Eq. (2).

		295K	100K
Li	x	0.000	0.000
	y	0.250	0.250
	z	0.125	0.125
	$U_{11}=U_{22}$	0.0202(24)	0.0163(35)
	U_{33}	0.0268(16)	0.0178(21)
	$U_{12}=U_{13}=U_{23}$	0.000	0.000
Tb	x	0.000	0.000
	y	0.250	0.250
	z	0.625	0.625
	$U_{11}=U_{22}$	0.0125(5)	0.0092(7)
	U_{33}	0.0110(3)	0.0089(4)
	$U_{12}=U_{13}=U_{23}$	0.000	0.000
F	x	0.2198(1)	0.2199(2)
	y	0.4119(1)	0.4107(2)
	z	0.4560(1)	0.4563(1)
	U_{11}	0.0182(3)	0.0127(4)
	U_{22}	0.0177(3)	0.0124(4)
	U_{33}	0.0172(3)	0.0127(4)
	U_{12}	0.0035(2)	0.0014(4)
	U_{13}	0.0040(2)	0.0016(3)
	U_{23}	0.0030(2)	0.0010(3)
	Extinction parameter $g = 3665$		
$R(F) = \frac{\sum NF_{\text{obs}} - E_{hkl} F_{hkl} }{\sum F_{\text{obs}}}$		3.6%	2.9%
$R_w(F) = \left(\frac{\sum w NF_{\text{obs}} - E_{hkl} F_{hkl} }{\sum w F_{\text{obs}}^2} \right)^{1/2}$		4.1%	3.3%

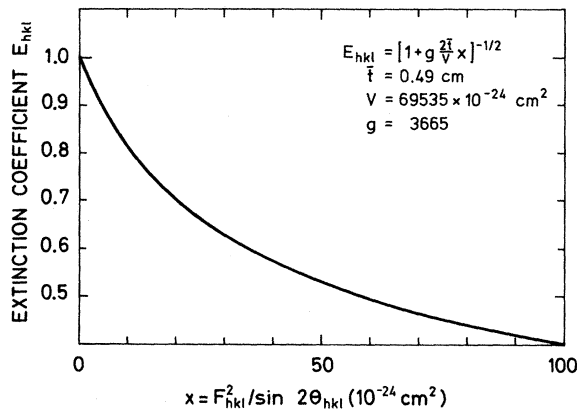


FIG. 1. Attenuation of the incident neutron beam when the crystal is in a Bragg reflection orientation implies that the integrated Bragg intensity is not proportional to $F_{hkl}^2/\sin^2 2\Theta_{hkl}$ but is attenuated by the extinction factor E_{hkl} . The curve is a best fit (see text) to 196 nonsymmetry-related reflections measured at 100 K.

TABLE II. Neutron scattering lengths of Li, Tb, and F as obtained from LiTbF_4 at 295 and 100 K compared to the recommended values from the Neutron Diffraction Commission, Ref. 16.

	LiTbF_4 (295K)	LiTbF_4 (100K)	NDC (Ref. 16)
Li	-0.204(5)	-0.199(7)	-0.214
Tb	0.760(5)	0.754(6)	0.76
F	0.567(4)	0.565(5)	0.55

Here β_j is 2.7 fm if site j is occupied by a Tb atom and zero for all other sites in the unit cell, $f(\vec{\tau})$ is the magnetic form factor of Tb,¹⁷ and in the last factor τ_z denotes the component of $\vec{\tau}$ along the c axis. The unit of μ is Bohr magnetons and we have omitted the indices h, k, l for brevity.

The *observed* intensities are influenced by extinction and the ratio of observed intensities below and above T_C becomes

$$\frac{I(T < T_C)}{I(T > T_C)} = \frac{(F_{hkl}^2 + F_{\text{mag}}^2)E(x_m)}{F_{hkl}^2 E(x_{hkl})} = \frac{x_m E(x_m)}{x E(x)}, \quad (5)$$

with $x_m = (F_{hkl}^2 + F_{\text{mag}}^2)/\sin^2 2\Theta_{hkl}$ and $x_{hkl} = F_{hkl}^2/\sin^2 2\Theta_{hkl}$.

The intensity ratio depends on the spontaneous magnetization μ , and using the data given in Table III and the extinction curve in Fig. 1 we have plotted the intensity ratio versus the spontaneous magnetization in Fig. 2 for the two Bragg points (0, 3, 1) and (0, 4, 0). The intensity ratio is measured experimentally, and from Fig. 2 we find the corresponding spontaneous magnetization. The results are given in Table IV.

It is worth noting that the contribution to the total integrated intensity from critical scattering is almost negligible because LiTbF_4 is a *dipolar-coupled* ferromagnet. As we have shown earlier the longitudinal wave-vector-dependent susceptibility $\chi(\vec{q})$ is very anisotropic in \vec{q} and in particular for \vec{q} along the c axis, as is the case in our Bragg peak scans, $\chi(0, 0, q)$ is *not* divergent at $T = T_C$ but passes through T_C at a small and almost constant value. However, due to the finite

TABLE III. Squared-structure factor over $\sin^2 2\Theta$ for nuclear scattering (column 2) and for magnetic scattering corresponding to 1 Bohr magneton on the Tb sites (column 3).

(h, k, l)	$F_{hkl}^2/\sin^2 2\Theta_{hkl}$	$F_{\text{mag}}^2 (1 \mu_B)/\sin^2 2\Theta_{hkl}$
(0, 4, 0)	7.902	1.255
(0, 3, 1)	3.944	0.867

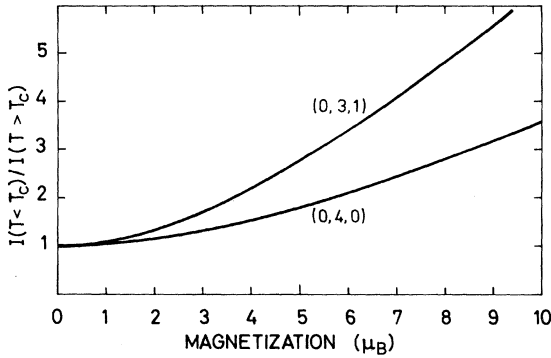


FIG. 2. Ratio of Bragg intensity below and above T_C depends on the spontaneous magnetization, the magnetic form factor, the Miller index, and the extinction. The dependence on magnetization is shown for the (0, 3, 1) and (0, 4, 0) reflections.

instrumental q -resolution one might pick up a small part of the divergent $\chi(q, 0, 0)$. This critical scattering contribution caused solely by instrumental resolution was just observable above T_C for the (0, 4, 0) reflection (see Fig. 3). In our study of critical scattering to be reported on separately we have found that $\chi(q, t_-) = \chi(q, t_+)$ if $t_- = \frac{1}{2}t_+$, with t_- and t_+ being the reduced temperatures $t_- = 1 - T/T_C$, $T < T_C$ and $t_+ = T/T_C - 1$, $T > T_C$. From the observed critical intensity cusp above T_C in Fig. 3 we can then derive the corresponding critical scattering below T_C as shown by the dashed line in Fig. 3. For the (0, 3, 1) reflection there was no sign of critical scattering above T_C , and it must therefore also be absent in the same scans below T_C .

C. Thermometry

The 7-mm-diam spherical crystal was held by two spring-loaded bowl-shaped aluminium pieces placed on the poles of the sphere. The top aluminium piece was thermally anchored to the bottom of a pot containing up to $\frac{3}{4}$ liter of liquid He. The sample holder was encapsulated in a thin-walled aluminium container with He gas in order to minimize temperature gradients. The temperature of the He bath in the pot was regulated by the pressure above the bath, and this pressure served as our primary temperature standard using the vapor pressure data of He as evaluated by Brickwedde *et al.*¹⁸

A secondary temperature standard used for monitoring the temperature during the measurements was furnished by a Ge cryoresistor. Around $T_C = 2.874$ K the sensitivity of the Ge cryo-

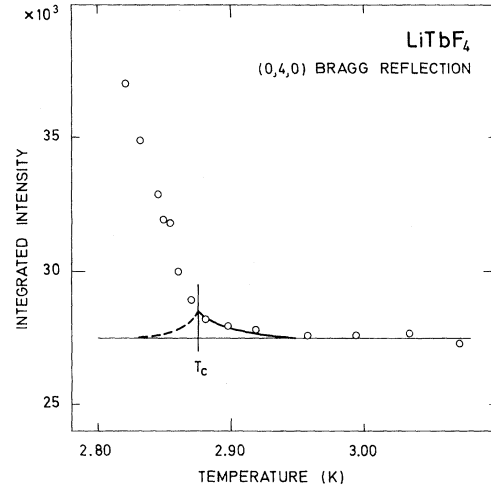


FIG. 3. Critical scattering in a q_z scan used to determine the integrated Bragg intensity is small and independent of temperature because LiTbF_4 is a dipolar-coupled uniaxial ferromagnet and $\chi(0, 0, q)$ is correspondingly small and temperature independent near T_C . The small cusp observed for $T > T_C$ for the (0, 4, 0) reflection is due to pickup of the divergent $\chi(q, 0, 0)$ due to the experimental resolution. The corresponding critical scattering contribution below T_C is given by the dashed curve.

resistor was 1 mK per 0.55 Ω and variations of the temperature exceeding 0.5 mK were readily observable.

The critical behavior of the spontaneous magnetization is given in terms of the reduced temperature $(T_C - T)/T_C$ and the main source of error in determining the reduced temperature originates from the determination of T_C .

Near T_C the magnetization $\mu(t)$ is expected to obey a power law

$$\mu(t) = \mu'(1 - T/T_C)^\beta, \quad (6)$$

and as will be discussed in Sec. III we have fitted our data to the power law, Eq. (6), with μ' , β , and T_C as free parameters. We found $T_C = 2.874 \pm 0.002$ K from the least-squares fit. This may be compared with $T_C = 2.86 \pm 0.03$ K from bulk magnetic susceptibility data.⁶ T_C can also be determined by the critical scattering versus temperature at a fixed small value of $\vec{q} = (q, 0, 0)$. Here q must be large enough to avoid any Bragg scattering contribution; in our case the smallest possible q was 0.06 \AA^{-1} . We found indeed a peak in the critical scattering at $T = T_C = 2.874$ K (see Fig. 4), but unfortunately the data are not accurate enough to provide a more accurate value of T_C than that obtained from the least-squares fit to a power law of the Bragg scattering data.

TABLE IV. Integrated intensity vs temperature for the (0, 4, 0) and (0, 3, 1) reflections. Above $T_C = 2.874\text{K}$ the scattering is purely nuclear, below T_C it is the sum of nuclear and magnetic scattering. The corresponding spontaneous magnetization in Bohr magnetons is also given.

(h, k, l)	T (K)	Integr. Int. (counts \AA^{-1})	Magnetization (μ_B)	Remarks
(0, 4, 0)	3.07	27 306		
	3.033	27 668		
	2.993	26 637		Nuclear scattering only
	2.9565	27 605		
	2.9185	27 832		
	2.896	27 984		
	2.8796	28 222		
	2.869	28 955-700	1.06	
	2.8595	30 011-400	1.64	
	2.853	31 785-250	2.21	
	2.848	31 933-100	2.28	
	2.8435	32 862 0	2.52	Critical region
	2.8298	34 864	2.94	
	2.821	37 041	3.34	
	2.797	40 222	3.86	
	2.774	42 459	4.19	
	2.755	44 414	4.46	
	2.732	46 774	4.78	
	2.627	55 194	5.82	
	2.591	57 729	6.11	
	2.5727	60 725	6.45	Approaching saturation
	2.457	63 897	6.80	
	2.382	66 359	7.06	
	2.2911	69 383	7.38	
	1.9427	77 701	8.23	
	1.7396	79 516	8.42	
(0, 3, 1)	3.07	14 324		
	3.032	14 308		
	2.994	13 967		Nuclear scattering only
	2.9565	14 369		
	2.939	14 256		
	2.9185	14 250		
	2.8962	14 483		
	2.8801	14 369		
	2.8691	15 665	1.27	
	2.86	17 330	1.81	
	2.8548	18 459	2.09	
	2.849	19 341	2.28	
	2.8442	20 472	2.51	Critical region
	2.8303	22 772	2.93	
	2.8138	25 778	3.40	
	2.795	29 603	3.94	
	2.775	31 724	4.22	
	2.754	34 516	4.57	
	2.733	36 157	4.76	
	2.625	47 153	5.98	
	2.59	49 911	6.27	
	2.528	53 026	6.59	Approaching saturation
	2.46	56 245	6.91	
	2.3745	60 089	7.29	
	2.2911	63 225	7.59	
	1.9427	72 463	8.48	
1.7396	75 556	8.77		

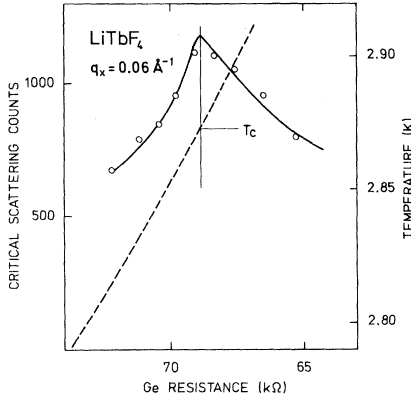


FIG. 4. Determination of T_C by critical scattering of fixed wave vector $\vec{q} = (0.06, 0, 0) \text{ \AA}^{-1}$. The dashed line gives the calibration curve of the Ge cryoresistor.

III. RESULTS

The integrated intensities of the (0, 4, 0) and the (0, 3, 1) Bragg reflections versus temperature are given in Table IV. The data in the critical region were fitted to the power law of Eq. (6) with μ' , T_C , and β as fitting parameters:

$$\begin{aligned} \mu' &= (19 \pm 1.5) \mu_B, \\ T_C &= 2.8741 \pm 0.0016 \text{ K}, \\ \beta &= 0.45 \pm 0.025. \end{aligned} \quad (7)$$

In the least-squares fit the data points were weighted accordingly to the Poisson uncertainty of the corresponding intensities. In the three-dimensional parameter space spanned by (μ', T_C, β) equiprobability parameter values form ellipsoids centered around the most probable point $(\mu', T_C, \beta) = (19, 2.874, 0.45)$. The stated uncertainties are the projections on the respective axes of the standard deviation ellipsoid.

The consistent values of μ derived from the (0, 4, 0) and the (0, 3, 1) reflections over the entire temperature interval strongly supports the reliability of the method we have used in converting Bragg intensities to magnetization. The magnetization versus temperature is compared to mean-field theory in Fig. 5 using the Brillouin function for $S = \frac{1}{2}$ and a saturation value of 8.9 Bohr-magneton. In Fig. 6 is shown the data in the critical region in a double-log plot illustrating the power law of Eq. (6).

It is emphasized that the extinction factor only varies by about 8% in the critical region and we may conclude that any conceivable systematic error in the extinction correction will lead to an error in β well within the uncertainty given in Eq. (7).

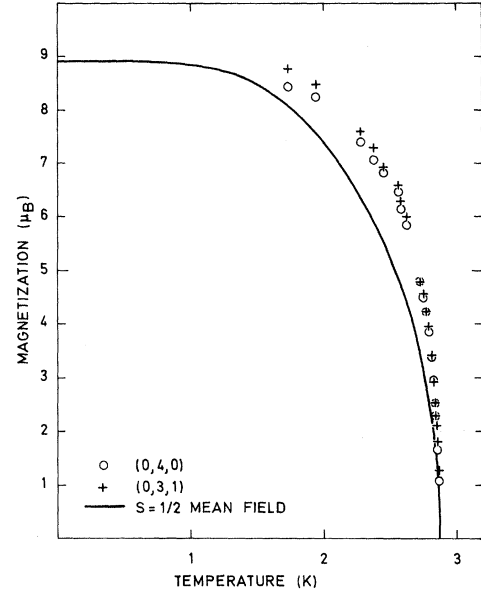


FIG. 5. Spontaneous ferromagnetic moment in LiTbF_4 as determined by Bragg scattering of neutrons.

IV. CONCLUSION

We have measured the spontaneous magnetization in the dipolar-coupled uniaxial ferromagnet LiTbF_4 by magnetic Bragg scattering of neutrons. Near the critical temperature, $0.001 < 1 - T/T_C < 0.03$, the reduced magnetization follows the power law

$$\mu(T)/\mu(0) = (2.13 \pm 0.17)(1 - T/T_C)^{0.45 \pm 0.03}. \quad (8)$$

This power law deviates quite significantly from that in Ising systems with short-range interactions only as, e.g., β -brass,¹⁹ where the amplitude is 1.6 and the exponent is 0.30.

Our value for β is close to the mean-field value of $\beta = 0.50$ as expected from the renormalization-

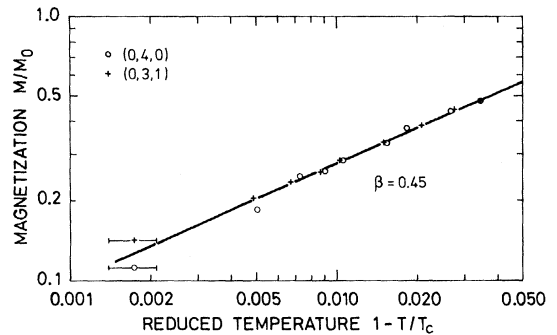


FIG. 6. Reduced magnetization M/M_0 vs. reduced temperature $1 - T/T_C$ in the critical region.

group analysis of Aharony.⁵ On the other hand our experimental value does deviate by two standard deviations from the mean-field value, and one might speculate why that is so.

We believe of course, that our quoted standard deviation is a reliable and conservative number, so the discrepancy between theory and experiment is real. The finite-exchange interactions imply in principle a crossover around a certain temperature T_{C_0} from short-range interaction Ising behavior to dipolar Ising behavior. The crossover temperature has been estimated by Aharony, and by inserting our values for the exchange interactions we find $T_{C_0} \approx 5T_C$, i.e., we are always in the dipolar regime in practice.

An alternative cause of the deviation of the critical exponents from mean-field values may lie in the finite splitting δ caused by the crystal field of the ideal ground-state doublet. Although

the splitting is small²⁰ ($\delta \approx 1.3$ K) it does prohibit ever so slightly the correlations to build up as they would in the ideal case. A theoretical (series-expansion) treatment²¹ of this problem in a *short-range* coupled Ising magnet gave the result that the critical indexes are probably not affected by the zero-field splitting (δ), so long as the spins order magnetically at a finite temperature. Whether this conclusion is valid also for a *dipolar-coupled* Ising magnet is an open question that may be answered by applying the renormalization-group theory. Finally we may suggest that the expected logarithmic deviations from mean-field behavior are strong enough to alter the effective critical exponents in the experimental temperature region—unfortunately it has not so far been possible to estimate the strength of the logarithmic deviation from theory or experiment.

*Work partly carried out while a guest scientist at AEC Research Establishment, Risø, Denmark.

¹L. P. Kadanoff, *Physics* **2**, 263 (1963); L. P. Kadanoff *et al.*, *Rev. Mod. Phys.* **39**, 395 (1967).

²K. G. Wilson, *Phys. Rev. B* **4**, 3174, (1971); **4**, 3184 (1971).

³K. G. Wilson and M. E. Fisher, *Phys. Rev. Lett.* **28**, 240 (1972).

⁴A. I. Larkin and D. E. Khmel'nitskii, *Zh. Eksp. Teor. Fiz.* **56**, 2087 (1969) [*Sov. Phys.-JETP* **29**, 1123 (1969)].

⁵A. Aharony and M. E. Fisher, *Phys. Rev. B* **8**, 3323 (1973); A. Aharony, *ibid.* **8**, 3363 (1973).

⁶L. M. Holmes, T. Johansson, and H. J. Guggenheim, *Solid State Commun.* **12**, 993 (1973).

⁷J. Als-Nielsen, L. M. Holmes, and H. J. Guggenheim, *Phys. Rev. Lett.* **32**, 610 (1974).

⁸L. M. Holmes, J. Als-Nielsen, and H. J. Guggenheim, preceding paper, *Phys. Rev. B* **12**, 180 (1975).

⁹M. Merisalo, M. H. Nielsen, and K. Henriksen, *Risø Report No. 279* (1973).

¹⁰R. E. Thoma, G. D. Brunton, R. A. Penneman, and T. K. Keenan, *Inorg. Chem.* **9**, 1096 (1970).

¹¹C. Keller and H. Schmutz, *J. Inorg. Nucl. Chem.* **27**,

900 (1965).

¹²M. S. Lehmann and F. K. Larsen, *Acta Crystallogr. A* (to be published).

¹³K. D. Rouse, M. J. Cooper, E. J. York, and A. Chakera, *Acta Crystallogr. A* **26**, 682 (1970).

¹⁴*International Tables for X-ray Crystallography* (Kynoch Press, Birmingham, 1968), Vol. III.

¹⁵W. H. Zachariasen, *Acta Crystallogr.* **23**, 558 (1967).

¹⁶G. E. Bacon, for The Neutron Diffraction Commission (1972); *Acta Crystallogr. A* **28**, 357 (1969).

¹⁷G. H. Lander, T. O. Brun, J. P. Desclaux, and A. J. Freeman, *Phys. Rev. B* **8**, 3237 (1973).

¹⁸F. G. Brickwedde, H. van Dijk, M. Durieux, J. R. Clement, and J. K. Logan, *J. Res. Natl. Bur. Stand. U. S.* **64A**, 1 (1960).

¹⁹J. Als-Nielsen and O. W. Dietrich, *Phys. Rev.* **153**, 717 (1967); D. R. Chipman and C. B. Walker, *Phys. Rev. B* **5**, 3823 (1972). O. Rathmann and J. Als-Nielsen, *ibid.* **9**, 3921, (1974).

²⁰I. Laursen and L. M. Holmes, *J. Phys. C* **7**, 3765 (1974).

²¹R. J. Elliott, P. Pfeuty, and C. Wood, *Phys. Rev. Lett.* **25**, 443 (1970).